

Response-based reliability contours for complex marine systems considering short and long-term variability

Seyffert, H. C.; Kana, A. A.

DOI

[10.1016/j.apor.2020.102332](https://doi.org/10.1016/j.apor.2020.102332)

Publication date

2020

Document Version

Final published version

Published in

Applied Ocean Research

Citation (APA)

Seyffert, H. C., & Kana, A. A. (2020). Response-based reliability contours for complex marine systems considering short and long-term variability. *Applied Ocean Research*, 103, Article 102332. <https://doi.org/10.1016/j.apor.2020.102332>

Important note

To cite this publication, please use the final published version (if applicable). Please check the document version above.

Copyright

Other than for strictly personal use, it is not permitted to download, forward or distribute the text or part of it, without the consent of the author(s) and/or copyright holder(s), unless the work is under an open content license such as Creative Commons.

Takedown policy

Please contact us and provide details if you believe this document breaches copyrights. We will remove access to the work immediately and investigate your claim.



Response-based reliability contours for complex marine systems considering short and long-term variability

H.C. Seyffert^{*,a}, A.A. Kana^a

Department of Maritime & Transport Technology, Delft University of Technology, the Netherlands

ARTICLE INFO

Keywords:

Response contours
Environmental contours
Reliability
Stiffened ship panel collapse
Rare responses
Combined loading
Short-term response variability
Long-term environmental variability

ABSTRACT

Evaluating marine system reliability requires considering the interaction of a limit state with the stochastic ocean excitation. Given a range of operational profiles, a relevant question is which sea states lead to the worst-case system responses, considering the effects of short and long-term variability. If the identified subset of operational profiles indeed leads to the worst-case system responses, it is possible to assess lifetime system performance without unnecessary computational effort via this directed set of conditions. Environmental contour methods identify rare sea states assumed to excite rare responses but generally do not include response dynamics when choosing these sea states. For systems with limit states involving combined loading or with multiple failure modes, rare environmental conditions may not exclusively lead to rare responses. In this case, the response cannot be severed from the identification of relevant sea conditions but should instead drive that identification. This paper illustrates a way to construct response-based reliability contours that identify sea states most relevant for analyzing rare responses of marine systems. These sea states are compared with sea states identified by environmental contours, showing the effect on perceived system risk levels when system dynamics, short-term response variability, and long-term environmental variability are considered.

1. Introduction

Due to the computational challenges associated with a long-term probabilistic analysis of marine systems, it is of major interest to identify relevant sea state conditions expected to most contribute to the long-term response. Examining such a subset of potential cases, versus all possible cases, allows a more in-depth analysis of the system response without spending unnecessary computational effort. Multiple methods exist to identify such sea states and generally rely on constructing environmental contours of the underlying excitation to identify rare environments which are assumed to excite equally rare system responses.

Environmental contours are very useful for identifying design parameter ranges with an approximate risk level in the initial design stages when relevant limit states are relatively unknown. But to identify the most relevant sea states to evaluate the reliability or performance of a system with a known or approximate limit state, other methods may give more meaningful results. This paper establishes such a method to construct contours of system reliability given a defined design lifetime, range of potential operational profiles, and limit state of interest for design purposes. Whereas environmental contours can be used to set design parameters based on the expected operational profile range, this

proposed method is geared towards evaluating that system by identifying a possible testing regime of sea states expected to lead to the worst-case system responses.

The paper is organized as follows. [Section 2](#) gives background on environmental contour methods to identify relevant sea states and offers a motivating example for a new method, which is developed in [Section 3](#). [Section 4](#) establishes a case study of identifying sea states which lead to the highest probability of stiffened ship panel collapse to illustrate the method. [Sections 5](#) and [6](#) examine how excluding the effects of long-term environmental variability and short-term response variability affect the perceived system reliability level. Finally, [Section 8](#) discusses the results and [Section 9](#) offers some conclusions.

2. Identifying relevant sea states

Environmental contour methods are often used in early design stages to identify operating conditions associated with a specific return period which can be used to give bounds on design parameters. The strength of the method is in its simplicity: the return period of a system response in a sea state is assumed to be completely defined by the return period of the associated contour of environmental parameters, e.g. significant wave height and a wave period to define a wave energy

* Corresponding author.

E-mail address: H.C.Seyffert@tudelft.nl (H.C. Seyffert).

<https://doi.org/10.1016/j.apor.2020.102332>

Received 10 October 2019; Received in revised form 17 June 2020; Accepted 10 August 2020

0141-1187/ © 2020 The Authors. Published by Elsevier Ltd. This is an open access article under the CC BY license (<http://creativecommons.org/licenses/by/4.0/>).

spectrum. In this way, the randomness inherent in the ocean environment is separated from the randomness of the structural response excited by that environment.

Many different approaches exist to define such contours, including, but certainly not limited to: the traditional Inverse First Order Reliability Method (IFORM) (Winterstein et al., 1993), the Inverse Second Order Reliability Method (ISORM) (Chai and Leira, 2018), a constant probability density approach (Haver, 1987), a direct Monte Carlo Simulation (MCS) sampling approach (Huseby et al., 2015), an importance sampling MCS approach (Huseby et al., 2014; Vanem, 2017), and defining contours by identifying highest density regions (Haselsteiner et al., 2017) or joint variable exceedances (Jonathan et al., 2014). A recent review of many such methods can be found in Ross et al. (2020). But regardless of the way the environmental contours are defined, a user still must eventually decide which sea states along that contour should be evaluated for a short-term analysis, see, e.g. Baarholm et al. (2010).

Other authors have examined response-based approaches to identify sea states associated with rare system responses, such as the coefficient of contribution method of Baarholm and Moan (2000). Relevant sea states for specific loading responses have also been identified along an environmental contour based on a representative spectral period that maximizes the load variance (Fukasawa et al., 2007) or by relating the environmental parameters of the contour to the load response via an analytical model (Winterstein et al., 1993). Vanem constructs and compares contours of extreme loading responses based on environmental parameters, but ignores short-term variability, using load response transfer functions which are solely functions of those environmental parameters (Vanem, 2017). Gouldby et al. similarly link environmental parameters to extreme overtopping rates of a flood defense structure via joint exceedance contours. This overtopping rate is described as a function of the extreme environmental parameters using response surfaces and a statistical wave emulator model (Gouldby et al., 2017). Other recent research has compared response-based and environmental contour-based approaches, e.g. Vanem and Guo (2019); Vanem et al. (2020); Wang et al. (2018).

For some marine structures, though, a relevant limit state to evaluate a system may not be so easily expressed as a function of the wave spectrum significant wave height and wave period. Additionally, it may be necessary to consider the short-term variability of a response within a given sea state to fully assess the system risk and performance. The challenge of accounting for the short and long-term variability while predicting extreme responses is discussed by Derbanne et al. (2017).

2.1. Motivating example

Such is the difficulty of identifying relevant sea states associated with rare system responses: effort is either focused solely on the excitation environment independent of the structure (as in most environmental contour methods) or solely on the structural response given a defined environment (as in, e.g. the dynamic IFORM approach offered by Lutes and Winterstein for load combination problems (Lutes and Winterstein, 2016)). But a relevant question for evaluating the performance or reliability of a marine system is: which sea states, each associated with a given probability of occurrence defined by either a wave parameter joint distribution or a sea state table, should be used to test the system? This question must be considered when defining testing regimes for marine systems, either for physical or numerical model tests.

As a motivating example, consider the collapse of a stiffened ship panel at a hull location which may be subject to sizable in-plane loading (due to global ship bending) and lateral loading (due to potential slam events), with a collapse limit state given in Fig. 1. In Fig. 1, the lateral load effect is on the y -axis while the in-plane load effect is on the x -axis. A detailed description of the process to define a panel collapse limit state is given in Hughes (1983). Stiffened panel failure is due to combined lateral and in-

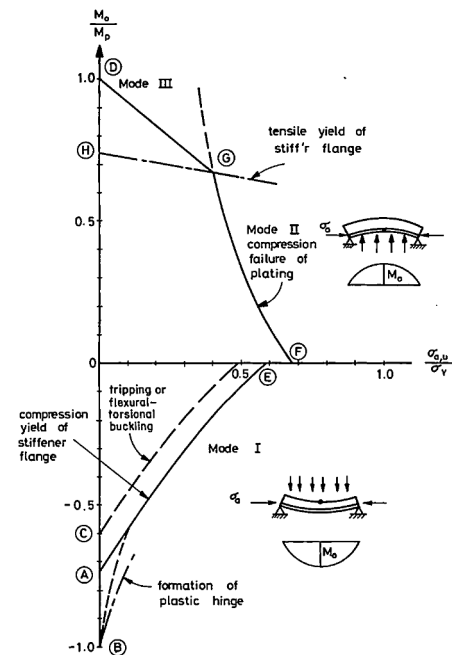


Fig. 1. Collapse of a stiffened panel due to lateral (y -axis) and in-plane (x -axis) loading effects (Hughes, 1983).

plane loading effects, both of which may be non-linear in nature. Panel failure may occur due to individual extremes of either load effect or due to a simultaneous moderate combination of both load effects. A lower-order reliability model for stiffened panel collapse due to combined loading was used in Seyffert et al. (2019b). That analysis examined panel reliability given a pre-defined operational profile representing a 1000-hour exposure to Hurricane Camille-type conditions. But that analysis did not consider the possibility that another sea state might have led to worse conditions for evaluating panel reliability. The effect of sea state harshness versus exposure time was further examined in Seyffert et al. (2019a), since the short-term variability of extreme loading values may be important to examine reliability due to combined loading effects.

This investigation furthers the work of Seyffert et al. (2019a) and lays out a rational way to identify sea states to evaluate system reliability or performance given a range of possible operational profiles, a defined lifetime exposure, and a limit state of interest. Further, the sea states identified by the resulting response-based reliability contours are compared to what results from a response-independent environmental contour approach and a brute-force simulation approach and the resulting effects on perceived system risk are discussed.

3. Method to define response-based reliability contours (RBRCs)

The aim of this method is to construct contours of a system response, here reliability (or conversely, failure probability), in all possible operational profiles while including the effects of short-term response variability and long-term environmental variability. Such contours can indicate which sea states lead to the worst-case responses over the system lifetime, allowing a more in-depth analysis of such operational profiles. These sea states are identified using a low-order reliability analysis based on extreme value theory and indicators of extreme behavior, meaning that any further high-fidelity but computation-heavy analyses can be focused solely on sea states expected to lead to the worst system responses.

Using indicators of extreme behavior links the stochastic excitation environment to rare load effects which contribute to rare system responses, similar to how load responses of interest are expressed as functions of the sea state parameters to identify relevant sea states in Winterstein et al. (1993), Vanem (2017) and Gouldby et al. (2017).

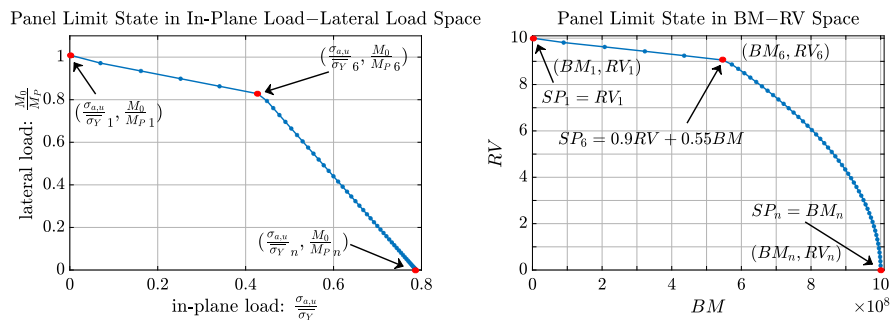


Fig. 2. Stiffened ship panel limit state described in the in-plane load - lateral load space (left) and in the BM - RV space (right).

Indicators of extreme behavior are defined as linear processes whose return-period extreme values are excited by inputs which are expected to similarly lead to return-period extreme values of a more complicated, potentially non-linear process. Given that the indicators are defined as linear processes, their return-period extreme values in a given sea state can be determined via extreme value theory, as described by Ochi (1990).

An indicator process may result from linearizing a non-linear process as in Kim et al. (2011), where the extreme response of linear vertical midship bending acts as an indicator for extreme responses of non-linear vertical midship bending. In that example, stochastic wave elevation profiles which excite return-period extreme linear vertical midship bending responses are expected to also excite extreme non-linear vertical midship bending responses. An indicator may also be a characteristic process not linearly related to the input/ output system but somehow related to the output extreme behavior, as in Seyffert et al. (2016). In Seyffert et al. (2016), extreme values of a linear moving average of a wave elevation profile are used to identify rare group-like behavior in the wave elevation, namely rare wave groups. In this case, the linear moving average process is an indicator to identify the occurrence of rare wave groups.

In both of the above cases (extreme linear vertical midship bending responses acting as an indicator for extreme non-linear vertical midship bending responses and extremes of a linear moving average of the wave elevation profile acting as an indicator for occurrences of rare wave groups) the indicator is a linear process defined independently of the sea state but that is also excited by the stochastic parameters, i.e. the stochastic wave excitation defined by the sea state parameters. No conditional distributions given the sea state are required to define indicators. Indicators may be defined by a range of methods, such as the pure linearization of a non-linear process as in Kim et al. (2011), or by more advanced approaches like the tail-equivalent linearization method (Fujimura and Kiureghian, 2007). The method to construct response-based reliability contours (RBRCs) expands on what was presented in Seyffert et al. (2019a). The steps are given with respect to the motivating example of stiffened ship panel collapse.

1. Identify indicators: For stiffened ship panel collapse due to combined lateral and in-plane loading effects, RBRCs can be constructed using the indicators identified in Seyffert et al. (2019b). The lateral and in-plane loading effects were described by non-linear functions of the stochastic relative velocity (RV) and bending moment (BM) acting at the panel location, based on the panel and ship dimensions and the stochastic wave excitation. Based on the analysis in Seyffert et al. (2019b), instances of extreme relative velocity and bending moment at the panel location were identified as good indicators of extreme lateral and in-plane loading effects on the panel, respectively. So in this case, the indicators are defined by linearizing the non-linear processes which govern the stiffened panel collapse. Of course, if the chosen indicators are not appropriate the resulting RBRCs will not give insight into which sea states are most relevant to evaluate the system response. But indeed this is also the case for defining

analytical response functions, response surfaces, or model emulators which attempt to link ocean environment with system responses. In any case, the resulting contours will only be useful if the indicators are truly representative of the desired non-linear extreme behavior.

2. Express limit state in the indicator space: The stiffened panel limit state illustrated in Fig. 1 is a non-linear function of the lateral and in-plane loading effects on the panel, which are themselves non-linear functions of the RV and BM acting at the panel location, respectively. Seyffert et al. employed a lower-order model of stiffened panel collapse using analytical expressions to relate the lateral and in-plane loading effects to the stochastic RV and BM excitation, based on stochastic wave excitation, and panel properties (Seyffert et al., 2019b). Such expressions allow a direct link between the excitation environment (waves, then RV and BM at the panel) and resulting load effects which then relate to panel failures via limit state exceedances. Given these analytical relationships, and that the limit state in Fig. 1 is one-to-one, the stiffened panel limit state can equivalently be written as a function of the RV and BM exciting the panel.

This modified limit state expresses instances of panel failure based on combinations of the indicators RV and BM. As an example, consider Fig. 2, which shows a stiffened panel limit state in the original in-plane - lateral load space in the left inset. The right inset shows this limit state expressed as a function of the BM and RV at the panel location.

3. Discretize indicator space limit state by a combined surrogate process: The limit states in the original load effect space and in the indicator space can be discretized by a finite number of points that span the entirety of the limit state, leading to the $(\frac{\sigma_{a,u}}{\sigma_y}, \frac{M_0}{M_{P_i}})$ and (BM_i, RV_i) for the $i = 1, \dots, n$ points in Fig. 2. Then, each point on the limit state in the BM - RV indicator space can be described by a combined surrogate process SP_i which is a weighted sum of the indicators BM and RV which correspond to the point (BM_i, RV_i) on the limit state in the BM - RV space. This combined surrogate process is described by Eq. (1):

$$\begin{aligned}
 SP_i &= \alpha_i RV + \beta_i BM \\
 \alpha_i &= \frac{RV_i}{\max(RV_1, \dots, RV_n)} \text{ for } i = 1, \dots, n \\
 \beta_i &= \frac{BM_i}{\max(BM_1, \dots, BM_n)} \text{ for } i = 1, \dots, n
 \end{aligned} \tag{1}$$

4. Choose a potential sea state: The RBRCs are defined using a cell-by-cell approach over all possible sea states. Therefore, the panel reliability is examined via a low-order reliability analysis in each potential sea state considering the combined lifetime exposure to that sea state. The possible sea states and the probability of encountering such a sea state may be defined by wave tables, as in IACS (2001), or by some joint distribution of sea state parameters, as in Bitner-Gregersen (2010). Based on the total design lifetime, plus any additional risk parameters, each sea state will then have an associated expected exposure period based on its probability of occurrence. Since considering a longer exposure can be equated to applying additional risk parameters to a shorter exposure, the long-term variability in this study is expressed by

the combined exposure to each sea state cell. In this particular example, the limit state is memoryless, so there are no cumulative effects related to the exposure length.

5. Relate extremes of the combined surrogate processes to failure probabilities: The desire now is to estimate the panel failure probability in the given sea state (with the lifetime exposure to this sea state defined by the probability of sea state occurrence) using extreme value theory and the definition of the limit state in the indicator space. As the combined surrogate processes, like in Eq. (1), are linear functions of the indicators BM and RV, which are linearly related to the Gaussian wave excitation, there exists a known extreme value distribution for each SP_i for the given sea state and exposure period. Comparing this extreme value distribution of the combined surrogate process with the limit state expressed in the indicator space gives a quick low-order reliability estimate. This reliability estimate is based on the probability that extreme values of SP_i over the given exposure exceed the limit state value at point i on the limit state in the BM - RV indicator space, as in Eq. (2):

$$p(\text{failure at point } i) = p(\text{fail}|SP_i) = p(SP_i > \hat{s}_{p_i}^*) \\ = 1 - \int_0^{\hat{s}_{p_i}^*} g(sp_{i,m}) \quad (2)$$

where

$$g(sp_{i,m}) = \text{extreme value distribution of the combined surrogate process } SP_i, \text{ given } m \text{ process cycles over the exposure to the given sea state} \\ \hat{s}_{p_i}^* = SP_i = \alpha_i RV_i + \beta_i BM_i = \text{value of combined surrogate process } SP_i \text{ at point } i \text{ on the limit state in the BM - RV indicator space}$$

Such a formula is similar to how Haver and Winterstein formulate a limit state based on comparing some critical response value with the most-likely extreme value of that response in a given sea state (Haver and Winterstein, 2008).

6. Relate conditional failure probabilities to overall failure probability in sea state: A method to relate the effects of extreme values of multiple stochastic processes and conditional probabilities similar to Eq. (2) to an overall failure probability given excitation from many potential combined surrogate processes SP_i is addressed in Seyffert (2018). The resulting probabilistic framework is used in Seyffert et al. (2019b) to efficiently estimate panel reliability in a given sea state by estimating how extreme values of the different surrogate processes SP_i are related over the exposure time. But in general, this overall failure probability estimate must be at least $p(\text{fail}|SP_i)$ for $i = 1, \dots, n$, given each possible combined surrogate process SP_i . This allows a quick estimate of the panel failure probability given an exposure to a single sea state, as in Eq. (3):

$$p(\text{fail}) = \text{maximum}(p(\text{fail}|SP_1), \dots, p(\text{fail}|SP_n)) \quad (3)$$

The failure probability estimate for a given sea state in Eq. (3) will be improved if the conditional failure probabilities from Eq. (2) are estimated via directed wave simulations, rather than the extreme value distribution estimate suggested by Eq. (2), as in Seyffert et al. (2019a). Such probabilities can be efficiently estimated by directed wave simulations by using response-conditioning wave techniques to construct an ensemble of waves expected to lead to rare load responses. However, the conditional failure probability estimates from Eq. (2) will be significantly more efficient than using simulations, allowing for a fast low-order reliability estimate in a given sea state.

7. Construct RBRCs using failure probabilities in each sea state: Steps 4–6 are repeated for each sea state cell and associated exposure time in the range of potential operational profiles. Then RBRCs can be assembled showing the estimated failure probability in all of the examined sea states, based on the sea state conditions, exposure period to each sea state, and the system limit state definition.

3.1. Inclusion of short-term response and long-term environmental variability

The defined procedure makes two major assumptions that distinguish it from environmental contour methods, apart from including the limit state in the identification of relevant sea states. First, this response-based reliability contour method identifies relevant sea states using their lifetime combined exposure. Based on the design lifetime and how the range of operational profiles are defined, each resulting sea state has an expected exposure duration. For the presented RBRC method, system reliability is examined in each sea state cell using the fraction of the lifetime exposure associated with that sea state. In this way, the long-term variability of the environmental condition is captured by the combined exposure time to each sea state cell, rather than by a return period associated with these sea conditions, as for environmental contour methods.

Generally in environmental contour methods, once relevant sea states are identified, they are used to test the system assuming a 3-hour storm duration, as suggested by, e.g. (DNV-GL, 2010; 2017; NOR, 2017). This 3-hr storm duration assumption may be appropriate for rare sea states, which will likely not be experienced for much longer than 3 h over a system's lifetime. But while this 3-hr storm duration assumption is physically realistic for the stationarity of the ocean environment, the system will experience the effects of many milder sea states for significantly longer over its lifetime. For systems subject to combined loading, where long exposures to milder sea states (the calm, versus the storm) can excite the moderate simultaneous loading that leads to failure, this 3-hr storm duration assumption may significantly under-predict the potential system risk. On the other hand, some sea states may be so rare that a 3-hr duration far exceeds the expected duration based on the design lifetime and applied risk parameters. Section 5 examines the effect of this 3-hr sea state duration (i.e. neglecting the long-term environmental variability) on the RBRCs and on the perception of the system risk.

Related to this storm duration limitation is the inclusion of short-term response variability. Again, most environmental contour methods assume there is no short-term response variability when constructing contours and identifying sea states. The short-term variability may be included when a sea state is used to test the system, again usually for a 3-hr duration. Section 6 examines how neglecting short-term response variability affects the identification of relevant sea states. Overall, while environmental contours are used to formulate design criteria, the RBRCs are meant to identify sea states which may be the most relevant for testing the reliability or performance of an already-formulated system, based on the long-term environmental variability and the short-term response variability.

4. Case study: stiffened panel collapse on the David Taylor Model Basin vessel 5415

The method to assemble RBRCs allows a designer to pinpoint sea states which are expected to lead to the worst-case system responses over all possible operational profiles for a specific design option. Again, this presents a subtle but important difference from environmental contour methods, where contours are defined independently of the design and can then be applied to multiple design alternatives. Whereas environmental contours can suggest sea states which may be interesting for general design options purely based on the rarity of the sea state, the RBRCs identify sea states expected to lead to the worst lifetime performance of a specific design option. This section furthers the motivational example presented in Section 2.1 by identifying relevant sea states to evaluate the probability of stiffened panel collapse on the David Taylor Model Basin (DTMB) vessel 5415, a modern destroyer-like hull with parameters given in Table 1.

Table 1
DTMB 5415 & stiffened panel particulars.

Parameter	Value
Overall length	151.18 m
Length on water line	142.18 m
Beam on water line	19.06 m
Draft	6.15 m
Displacement	8424.4 m ³
Block Coefficient	0.507
Longitudinal Center of Buoyancy (% Lpp fwd +)	-0.683
Panel Location (fwd of midships +)	13.96 m
Panel Deadrise Angle	4°
Web frame spacing	1905 mm
Plate/ Stiffener Yield Stress	330 MPa
Steel Young's modulus, E	190 GPa

4.1. Range of operational profiles

For this analysis the range of operational profiles is defined by wave data measured between 1989–2008 in the North Atlantic. The possible wave spectral parameters, significant wave height H_s and wave zero-crossing period T_z , can be expressed via a 3-parameter Weibull distribution, as from Bitner-Gregersen (2010). This wave data was previously used to assemble environmental contours in Vanem and Bitner-Gregersen (2012) and Huseby et al. (2013). Parameters to define the joint distribution for this North Atlantic region, defined by Bitner-Gregersen (2010), are given in Table 2. These parameters describe a modified marginal distribution of the significant wave height in Eq. (4) based on the long-term wave climate and will be used for a 2-parameter $H_s - T_z$ Bretschneider spectrum.

$$\begin{aligned}
 f_{H_s, T_z}(h, t) &= f_{H_s}(h) f_{T_z|H_s}(t|h) \\
 f_{H_s}(h) &= \frac{\beta}{\alpha} \left(\frac{h-\gamma}{\alpha}\right)^{\beta-1} \exp\left(-\left(\frac{h-\gamma}{\alpha}\right)^\beta\right) \quad h \geq \gamma \\
 f_{T_z|H_s}(t|h) &= \frac{1}{\sigma(h)t\sqrt{2\pi}} \exp\left(-\frac{(\ln(t)-\mu(h))^2}{2\sigma(h)^2}\right) \quad t > 0
 \end{aligned}
 \tag{4}$$

where

$$\begin{aligned}
 \mu(h) &= E[\ln(t)|H_s = h] = a_1 + a_2 h^{a_3} \\
 \sigma(h) &= std(\ln(t)|H_s = h) = b_1 + b_2 \exp(b_3 h)
 \end{aligned}$$

Stiffened ship panel reliability is examined for a 30-year design lifetime with a probability of non-exceedance $PNE = 0.90$ for the most-likely extreme responses, resulting in an effective 300-year effective exposure. This effective exposure can be determined via linear extreme value theory, see, e.g. Ochi (1990), where the extreme value distribution, $g(y_m)$, of a linear process y with probability density function f_Y and cumulative density function F_Y is defined in Eq. (5) by the number of cycles m expected over a given exposure period. The most probable extreme value of the random process y over the m cycles, \bar{y}_m , is related to m in the limit as $m \rightarrow \infty$ by Eq. (7).

$$g(y_m) = m f_Y(y_m) \{F_Y(y_m)\}^{m-1}
 \tag{5}$$

Table 2
North Atlantic distribution parameters for Eq. (4) from (Bitner-Gregersen, 2010).

Parameter	Value		
	α	β	γ
	1.094	1.213	0.329
	$i = 1$	$i = 2$	$i = 3$
a_i	1.060	0.653	0.405
b_i	0.020	0.408	-0.784

$$\left. \frac{d}{dy_m} g(y_m) \right|_{\bar{y}_m} = 0
 \tag{6}$$

$$\frac{1}{m} \approx 1 - F_Y(\bar{y}_m)
 \tag{7}$$

An issue of using the most probable extreme value \bar{y}_m as a design value for engineering purposes is that \bar{y}_m has about a 63.2% probability of exceedance over the m cycles. Therefore, a risk parameter α_r can be applied. Then, there is an extreme value \hat{y}_m that satisfies Eq. (8)-(9):

$$\int_0^{\hat{y}_m} g(y_m) dy_m = \{F(\hat{y}_m)\}^m = 1 - \alpha_r
 \tag{8}$$

$$1 - F_Y(\hat{y}_m) = \frac{\alpha_r}{m}
 \tag{9}$$

The formulation of Eq. (9) allows the definition of an extreme value \hat{y}_m associated with an exposure (which can be expressed by the number of cycles or samples m) and a risk parameter α_r . The risk parameter α_r is used to define the response whose most-likely extreme value over a given exposure has the defined probability of non-exceedance $PNE = 1 - \alpha_r$. In this case then, a 30-year lifetime with a probability of non-exceedance $PNE = 0.90$ can equivalently be expressed as a 300-year effective exposure by Eq. (9).

This 300-year effective exposure and the distribution parameters from Bitner-Gregersen (2010) determine the fraction of the lifetime exposure devoted to each sea state cell, given a 0.25 meter \times 0.25 second cell dimension, as illustrated in Fig. 3. As a cut-off, any sea state cell whose combined lifetime exposure is less than 1 min is not considered to occur (i.e. has a 0-hour exposure). This is done because the method to construct the RBRC's in Section 3 uses the most-likely extreme values of the linear indicators based on extreme value theory, which as noted above for Eq. (7), is only valid as the extreme values become large. Considering that the possible wave periods range from 3.5s to 11.5 s, this 1-minute cutoff ensures that a sufficient number of wave cycles are experienced in each sea state cell to satisfy the assumptions of extreme value theory. Practically speaking, this cutoff means that about 14.3 min of the 300-year effective exposure are neglected. These 14.3 min of neglected exposure time are spread over 734 sea state cells, where the average exposure time of the neglected sea state cells is 1.17 seconds.

Given the exposure to each sea state, the RBRCs can identify the most relevant sea states for evaluating the reliability of a given panel design, based on the tradeoff between the sea state harshness and the exposure time expected in that sea state.

4.2. DTMB 5415 stiffened panel design

This paper examines three potential stiffened panel design options for the inner bottom external shell strake of the DTMB 5415. The 17th International Ship and Offshore Structures Congress (committee V.5 Naval Ship Design) used existing naval structural rules from 6 different classification societies to determine an optimal stiffened panel for the DTMB 5415 (Ashe et al., 2009). Three panel designs are used for this analysis with properties given in Table 3. As in Seyffert et al. (2019a,b) only mode 2 and 3 panel failures are considered, relating to the top quadrant of Fig. 1.

4.3. Stiffened panel RBRCs

Using the process described in Section 3 and the potential operational profiles described by Eq. (4) and Table 2, RBRCs are assembled for the panels. As described in Seyffert et al. (2019b), extreme relative velocity (RV) at the panel location is used as an indicator for extreme lateral loading effects on the panel. In the same way, extreme global bending moment (BM) at the panel location is used as an indicator for extreme in-plane loading effects on the panel. The estimation of the

Table 3
Stiffened panel designs for the DTMB 5415 from (Ashe et al., 2009).

	Panel A	Panel B	Panel C
Stiffener Design Pressure [kPa]	103.6	60.6	59.75
Web Design Pressure [kPa]	103.6	33.6	33.89
Plate Thickness [mm]	11	9	8.1
$H_{web} \times T_{web}$ [mm]	150×9	160×6.2	154.4×6
$H_{flange} \times T_{flange}$ [mm]	90×14	120×9.8	101.8×8.9
Stiffener Spacing [mm]	700	672	500
Bottom Cross-Section Modulus [m^3]	4.60	3.77	4.14
Longitudinal Structure Weight [kg]	21,121	16,520	19,276

failure probability for the panels in Seyffert et al. (2019b) was quite accurate and efficient compared to brute-force Monte Carlo Simulations, indicating that the choice of these indicator processes is appropriate for the non-linear loading models. Using these linear indicators maintains a clear connection between extreme ocean environments (sea spectrum defined by $H_s - T_z$), extreme indicator responses (RV and BM at the panel location), and characteristics which impact panel reliability (interaction of lateral and in-plane loading effects with the limit state definition), leading to the RBRCs in Fig. 4. These contours were generated in less than 30 s on a MacBook Pro-personal laptop, 2.3 GHz Intel Core i5.

The contours in Fig. 4 indicate that all panels have a similar range of sea states that lead to appreciable failure probabilities which runs from about $H_s = 3.5m - T_z = 4.5s$ to about the $H_s = 8.5m - T_z = 8.5s$ sea state. For all panels, the worst performances are clustered from the $H_s = 4.5m - T_z = 5.5s$ to $H_s = 5.5m - T_z = 6.5s$ sea states. Overall, Panel A has the best performance, i.e. the lowest collapse probabilities, followed by Panel B and then Panel C.

5. Effect of long-term environmental variability

When a sea state is chosen using environmental contour methods, this sea state is generally used to test the system assuming a 3-hr storm duration, as recommended by, e.g. (DNV-GL, 2010; 2017; NOR, 2017). While this limited 3-hr exposure reflects physical limits on sea state stationarity for storm conditions, from a statistical side it neglects the combined effects on a system over its lifetime exposure to a potential sea state. Especially for combined loading problems where simultaneous moderate loading can lead to interesting system responses, assuming only a 3-hr sea state duration may significantly under predict the potential risk from a sea state excitation. But on the other hand, this 3-hr storm duration may inflate the importance of sea states that are in reality much rarer when considering the design lifetime and applied risk parameters, potentially leading to over-conservative designs.

Fig. 5 gives the RBRCs for the panels using the procedure from Section 3 but assuming that each considered sea state has a 3-hr duration. In this case, the long-term variability of each sea state cell is

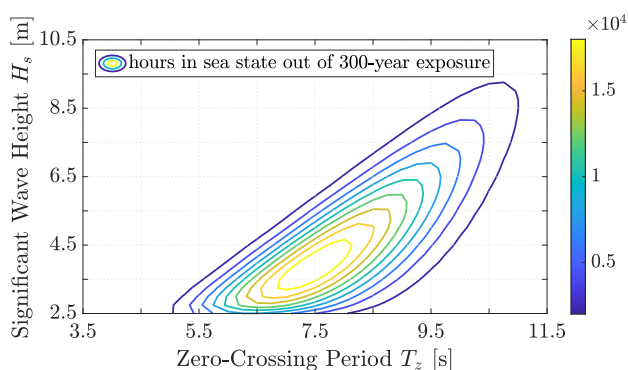


Fig. 3. Hours in each North Atlantic sea state ($H_s - T_z$) out of 300-year effective exposure.

neglected. This test is equivalent to seeking sea states which will lead to the worst response in a 3-hr duration, regardless of the rarity of that sea state. Also included in Fig. 5 are the RBRCs which do include the long-term environmental variability (i.e. Fig. 4) in light grey to better compare the location of the resulting contours.

In this case, the RBRCs neglecting long-term environmental variability by assuming a 3-hr sea state duration generally range from $H_s = 4m - T_z = 4s$ to about the $H_s = 8.5m - T_z = 7.5s$ sea states, are much narrower and shifted towards higher significant wave heights and lower zero-crossing wave periods, and overall have much higher failure probabilities than the contours in Fig. 4. The higher failure probabilities for all panels can be attributed to the constant 3-hr sea state duration. The sea states leading to the highest failure probabilities for each panel in Fig. 5 (neglecting long-term environmental variability) are considerably rarer in the 300-year effective exposure than what the constant 3-hr sea state duration suggests. For all panels, the constant 3-hr storm duration assumption indicates that the $H_s = 5.0m - T_z = 5.0s$ sea state is the most relevant. Based on the wave parameter model described in Section 4.1 which includes long-term environmental variability, this sea state would only be expected to occur for about 1.4 minutes out of the 300-year effective exposure (as in Fig. 4), far less than the 3-hr duration assumed in Fig. 5.

This disparity indicates the need for engineering judgment when considering allowable risk profiles and choosing relevant sea states for testing regimes based on that risk profile. Assuming a 3-hr sea state duration is a reasonable choice and is common practice, as evidenced by its codification in classification society rules. But it could lead to an over-conservative design, as might happen in this case. Based on the failure probability contours in Fig. 5, none of the panel designs could be considered acceptable. However, the worst-case sea states identified by Fig. 5 are likely to occur for a far shorter duration than 3-hr over the 300-year effective exposure when considering the long-term environmental variability.

Note that this $H_s = 5.0m - T_z = 5.0s$ sea state would have a 3-hr duration when considering long-term environmental variability if the original 30-year design lifetime was paired with a probability of non-exceedance $PNE = 0.9992$ (based on Eq. (8)-(9)). This is clearly a very different risk profile than the 30-year design lifetime with a probability of non-exceedance $PNE = 0.90$, which gives the contours in Fig. 4. This further implies that the constant 3-hr sea state durations leading to the reliability contours in Fig. 5 could all be obtained based on the original 30-year design lifetime with different applied risk parameters for each sea state, though that makes comparing the performance of the panels in different sea states certainly more challenging. It may be more judicious to judge a design based on its response when considering the long-term environmental variability paired with a universal explicitly-defined risk profile. This allows a designer to specify any desired risk profile and judge a design's performance accordingly, rather than designing for a sea state which is far rarer than what the designer is concerned about or comparing design responses associated with different risk profiles.

6. Effect of short-term response variability

The RBRCs in Fig. 4 give a clear picture of the panel performance in each potential sea state with exposures defined by the wave model from Eq. (4) and Table 2 because the panel limit states are known. But for many problems, there may not be a known limit state, or it may not be so simply defined as to be implemented in the procedure in Section 3. These limitations are what make the environmental contour methods presented in Section 2 so appealing. Since environmental contours only include the rareness of a sea state, no limit state information is necessary. Response-based methods add information on the system dynamics, but still at a low level of system detail. Considering the design limit state is closely connected to including the effects of short-term variability. Assuming there is no short-term variability essentially boils

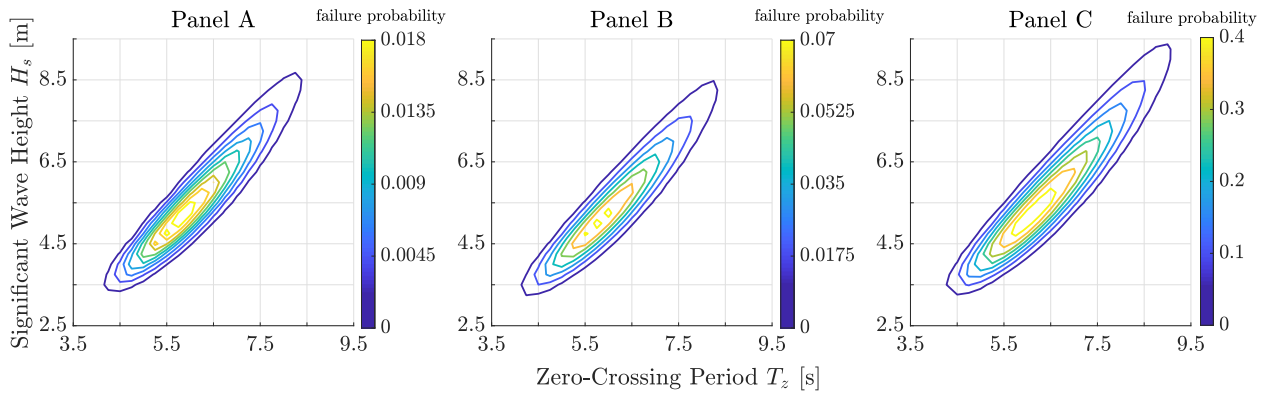


Fig. 4. Failure (collapse) probability contours of panels A, B, and C with sea state duration given by Fig. 3 (considering long-term environmental variability and short-term response variability).

the system response down to a single value given the sea state excitation, e.g. a most-probable extreme value, as noted by Derbanne et al. (2017). Depending on how this value is calculated, it may not have any relation to the design limit state, especially for a system with a limit state including multiple failure modes.

The question then is, if a designer has an idea of relevant loading effects for system performance, but no limit state definition, can relevant sea states still be identified using the idea of the method presented in Section 3? Consider that rare system responses are likely due to rare loading effects on the system. Instead of using environmental contours to identify rare sea states, and assuming that such sea states excite equally rare responses, the theory of Section 3 can be adapted to identify sea states that excite the most-likely extreme load effects, again using a cell-by-cell approach and extreme value theory.

In each sea state cell, the most-likely extreme relative velocity and bending moment at the panel location can be approximated based on the exposure using extreme value theory. Contours of the most-likely extreme relative velocity and bending moment responses at the panel location, given the sea state parameters and cell exposure time, are shown in Fig. 6. Note that the contours in both insets have a rugged appearance in the top left region. This is due to the 1-minute exposure cutoff referenced in Section 4.1, where sea state cells with an expected exposure of less than 1-minute over the entire 300-year effective exposure are not considered. Again, that choice was made to reflect the assumptions of the extreme value theory used in Eq. (5)–(7), where the expressions to calculate the most-likely extreme value are only valid as that value becomes large. Therefore, the rugged border of the contours in Fig. 6 reflects the boundary between sea states which are and are not expected to occur.

These contours illustrate how relevant sea states might be identified if short-term variability is ignored, as the contours in Fig. 6 only give

the most-likely extreme load value at each sea state cell, whereas the RBRCs in Fig. 4 include the effects of short-term variability based on the limit state by Eq. (2). Identifying sea states via these contours is similar to the coefficient of contribution method adopted by Baarholm and Moan (2000).

The left inset of Fig. 6 gives the most-likely extreme relative velocity response at the panel location, while the right inset gives the most-likely extreme bending moment response at the panel location based on Eq. (6), given the sea state and exposure. Fig. 6 does give some insight into which sea states are most relevant for panel reliability, especially considering the contours of most-likely extreme relative velocity at the panel location. The contour region with the highest relative velocity values at the panel location corresponds with the region of higher failure probabilities for all the panels. In Seyffert et al. (2019b), it was found that the panels were more vulnerable to failures due to extreme lateral load effects (whose indicator is extreme relative velocity at the panel location) than failures due to extreme in-plane load effects (whose indicator is extreme bending moment at the panel location), explaining why sea states corresponding to high most-likely extreme relative velocity responses at the panel location indicate relevant sea states for panel performance. In contrast, sea states leading to the most extreme bending moment responses at the panel location do not correspond with sea states that lead to appreciable failure probabilities.

7. RBRC sea states compared to IFORM environmental contours and MCS

Fig. 4 gives contours of the panel failure probability based on the contribution of each sea state cell to the entire 300-year effective exposure. From these contours, specific sea states can be identified which are expected to excite the highest failure probabilities for the panels. An

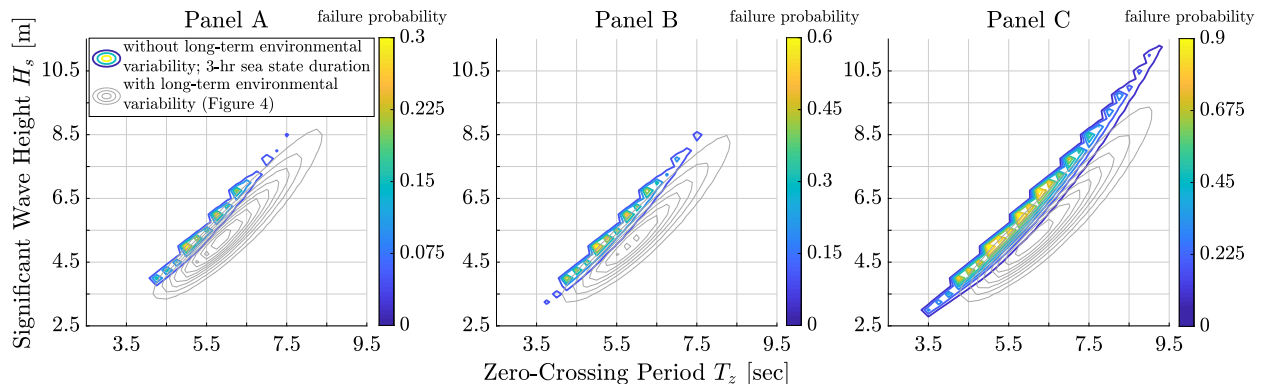


Fig. 5. Response-based reliability contours of panels A, B, and C assuming a 3-hr sea state duration (i.e. neglecting long-term environmental variability), along with RBRCs that include the long-term environmental variability from Fig. 4 in light grey.

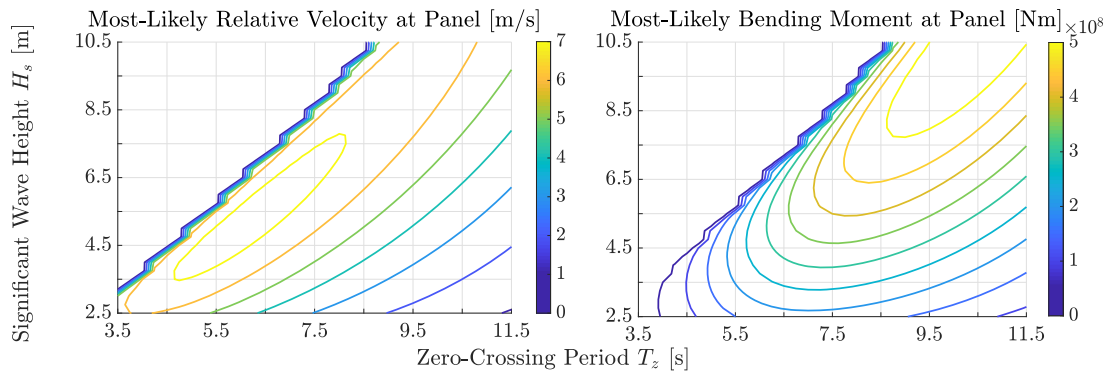


Fig. 6. Left inset: Most-likely extreme relative velocity (RV) [m/s], right inset: most-likely extreme bending moment (BM) [Nm] at panel location (i.e. neglecting short-term response variability).

important question is then: which sea states would be identified as relevant if an environmental contour approach were used? This can help illustrate whether the major assumption of environmental contours: that rare sea states are directly linked to rare system responses, is appropriate for such a system as stiffened panel collapse due to combined loading effects. For this comparison, environmental contours associated with 300-year, 30-year, and 10-year return periods are constructed using the Inverse First Order Reliability Method (Winterstein et al., 1993), without including any short-term response variability.

The IFORM contours for this comparison do not include the panel response variability because even the simple collapse model presented in Section 3, which allows for multiple failure modes and combined loading, is too complicated to be expressed solely as a function of the sea state parameters H_s and T_z . In general, the omission of the short-term variability is handled by inflating the IFORM contours based on FORM omission factors, as suggested by DNV-GL (2010). Winterstein et al. note that “if the expected largest value of the worst q-probability sea state (of duration d) is taken as an estimate for the long term q-probability response, the target value is underestimated by about 10% or more,” where the q-probability response is the desired load probability of exceedance value which defines the sea state (Winterstein et al., 1993).

This issue is generally resolved by inflating the IFORM to look for rarer responses, but there is no easy way to determine the magnitude of the required safety factor to account for the simplification. Winterstein et al. acknowledge that the proper inflation factor is structure-dependent, and the correct choice of this factor may require in-depth numerical or physical mode tests, as in Baarholm et al. (2010). Such an inflation factor may be strongly structure-dependent, and for different structural problems IFORM inflation factors have been chosen ranging from 0.57 (Sødahl et al., 2006) up to 0.98 (Haver and Kleiven, 2004). In general though, only the full probabilistic analysis can indicate the “correct” inflation factor for the problem at hand.

As a benchmark of which sea states are most relevant, brute force Monte Carlo Simulations (MCS) are conducted for a test grid of sea states. At each sampled sea state cell, 500 MCS are carried out for the sea state duration given by Fig. 3. The MCS include the long-term environmental variability via the lifetime combined exposure to each sea state and the short-term response variability via stochastic wave simulations testing the panels for the exposure using the higher-order panel collapse model presented in Seyffert et al. (2019b). The test grid of the sea states examined by MCS, along with the 300, 30, and 10-year IFORM contours are given in Fig. 7. The MCS test points are chosen to overlap with similar regions of the contours in Figs. 4–5, relevant sea states from the insets of Fig. 6 (highest most-likely relative velocity and bending moment extreme values), and the intersection of the contours in Fig. 6 with the IFORM contours. This grid of sea states leads to failure probability contours from the MCS shown in Fig. 8. The RBRCs from

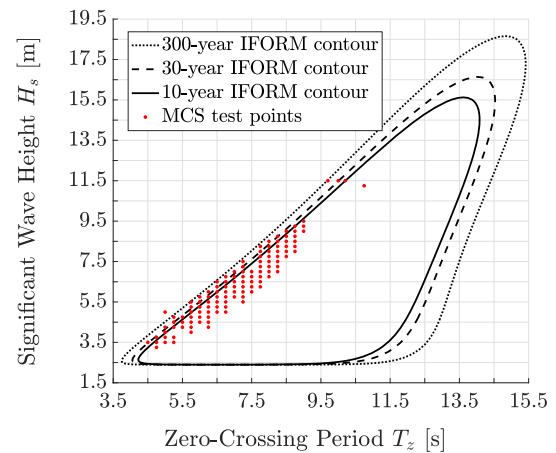


Fig. 7. Testing grid for MCS analysis, along with 300-year, 30-year, and 10-year IFORM contours.

Fig. 4 are also plotted in light grey to better compare the location of the contours. The MCS were run on an Ubuntu desktop with 12x Intel(R) Xeon(R) CPU E5-2609 v3 @ 1.90 GHz, for a total of 12.45 hours of computation time.

The failure probability contours from the MCS in Fig. 8 show a strong similarity with the RBRCs shown in Fig. 4 assembled by the method in Section 3 based on the range of sea states leading to appreciable and significant failure probabilities. This is impressive considering that the RBRCs in Fig. 4 come from a low-order reliability model based on extreme value theory, and require only 30 s of computation time to generate. In contrast, the MCS test the panel response excited by stochastic wave excitation time simulations based on the exposure to each sea state and use a higher-order panel collapse model involving combined non-linear loading effects, requiring about 12.45 h of computation time. Ranges of appreciable failure probabilities from the MCS are found in sea states that range from $H_s = 3.5\text{m} - T_z = 4.5\text{s}$ to about $H_s = 8.5\text{m} - T_z = 8.5\text{s}$ and it is similarly found that Panel A overall has the best performance followed by Panels B and then C.

For Panel A, the sea state with the highest failure probability identified by the RBRCs in Fig. 4 is the same sea state indicated by MCS that leads to the highest failure probabilities: $H_s = 5.0\text{m} - T_z = 5.75\text{s}$. Panels B and C similarly pinpoint sea states which are confirmed by MCS to lead to very high failure probabilities. These results indicate that the sea states identified by the method in Section 3 can indeed be taken as a range of sea states which are expected to lead to the worst-case panel responses. This can have a major impact for designing testing regimes for a system, where choosing relevant sea states is important to effectively and efficiently test the lifetime performance of a system.

Table 4 compares the sea states identified by the MCS in Fig. 8, the

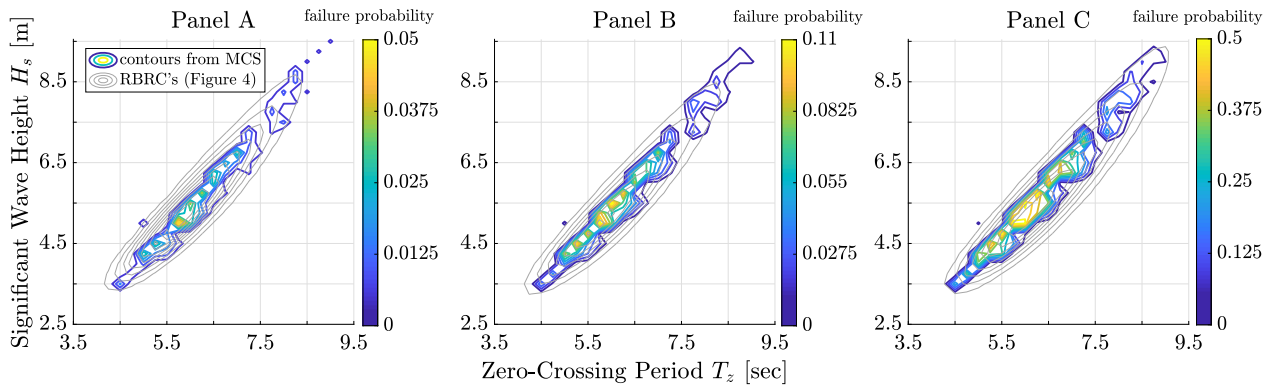


Fig. 8. Failure probability contours assembled by 500 MCS at each sea state cell (considering long-term environmental variability and short-term response variability), along with RBRCs from Fig. 4 in light grey.

RBRCs in Fig. 4, the RBRCs assuming a constant 3-hr sea state duration in Fig. 5, sea states identified by maximized relative velocity and bending moment at the panel location, as in Fig. 6, and sea states identified by the intersection of the IFORM environmental contours and the relative velocity and bending moment contours from Fig. 6. The major point of comparison is whether a method identifies sea states which indeed lead to the worst-case panel responses, as compared to MCS.

The first 5 rows in Table 4 give the sea state expected to lead to the maximum failure probability for each panel design, based on each particular method. The first row is the benchmark as it gives the sea state from the 500 MCS, based on the examined sea state cells from Fig. 7, which leads to the highest failure probability for each panel design. The second row gives the sea state leading to the highest failure probability for each panel from the RBRCs in Fig. 4. The third row gives this sea state based on the RBRCs assuming a constant 3-hr sea state duration, from Fig. 5. The fourth row identifies the sea state leading to the largest most-likely extreme relative velocity response and the fifth row identifies the sea state leading to the largest most-likely extreme bending moment responses at the panel location.

Following are three blocks of two rows, corresponding to examining sea states associated with the 300-year, 30-year, and 10-year IFORM contours. For each block, the rows give the sea state along the N-year IFORM contour associated with the largest most-likely extreme relative velocity response and bending moment response at the panel location.

For each panel block, the first column gives the maximum failure probability found by the particular method for the given panel (if the method returns a failure probability), with the associated sea state significant wave height H_s and zero-crossing period T_z in the second and

third columns. The fourth column ' $p_{fail}/p_{fail,max}$ ' gives the ratio of the MCS failure probability at the identified sea state to the maximum MCS failure probability for that panel over all examined sea states. This ratio shows whether a sea state identified by a particular method actually leads to the worst-case system response if the system were examined via a higher-fidelity model taking into account both long-term environmental variability and short-term response variability, such as MCS. This will affect the perceived risk level because if an engineer chooses a sea state thinking it leads to the worst possible response, but in reality there is another sea state which leads to a worse response, the perception of the system risk will be skewed.

8. Discussion

Table 4 indicates that the RBRCs considering both long-term environmental variability and short-term response variability give a very accurate identification of the most relevant sea states for stiffened panel failure, based on the failure model used here. For all panels, the RBRC-identified sea state would lead to a failure probability that is at least 95% of the maximum possible failure probability identified by brute-force MCS. In addition, comparing Figs. 4 and 8 indicates that the RBRCs identify the region of sea states which leads to the highest failure probabilities for each panel design. Such low-order RBRCs can be useful when defining a testing profile regime for a complex marine system which will be tested by some higher-fidelity model.

Assuming a constant 3-hr sea state duration (i.e. Fig. 5) strongly diminishes the likelihood that the identified sea state leads to the worst-case panel response when compared to MCS which include that long-term environmental variability. Note that the failure probabilities in

Table 4
Comparison of identified sea states & expected failure probabilities from different methods.

method	Panel A				Panel B				Panel C			
	max. p(fail)	H_s [m]	T_z [s]	$\frac{P_f}{P_{f,max}}$	max. p(fail)	H_s [m]	T_z [s]	$\frac{P_f}{P_{f,max}}$	max. p(fail)	H_s [m]	T_z [s]	$\frac{P_f}{P_{f,max}}$
MCS	0.05	5.0	5.75	1.0	0.118	5.5	6.0	1.0	0.536	5.75	6.25	1.0
RBRC	0.020	5.0	5.75	1.0	0.075	5.0	5.75	0.97	0.436	5.0	6.0	0.95
3-hr RBRC	0.330	5.0	5.0	0.16	0.671	5.0	5.0	0.10	0.972	5.0	5.0	0.10
Most-Likely RV	-	5.0	6.0	0.60	-	5.0	6.0	0.64	-	5.0	6.0	0.95
Most-Likely BM	-	11.25	10.75	0	-	11.25	10.75	0	-	11.25	10.75	0.01
300-yr IFORM + Most-Likely RV	-	4.5	5.0	0.004	-	4.5	5.0	0.0064	-	4.50	5.0	0.006
300-yr IFORM + Most-Likely BM	-	11.5	9.7	0.12	-	11.5	9.7	0.068	-	11.5	9.7	0.041
30-yr IFORM + Most-Likely RV	-	4.5	5.25	0.59	-	4.5	5.25	0.90	-	4.50	5.25	0.90
30-yr IFORM + Most-Likely BM	-	11.5	10.0	0	-	11.5	10.0	0	-	11.5	10.0	0.026
10-yr IFORM + Most-Likely RV	-	5.0	5.75	0.90	-	5.0	5.75	0.88	-	5.0	5.75	0.90
10-yr IFORM + Most-Likely BM	-	11.5	10.2	0	-	11.5	10.2	0.05	-	11.5	10.2	0.02

Fig. 5 are significantly higher than what is predicted by the RBRCs in Fig. 4 or the brute-force MCS in Fig. 8. This is because each sea state in Fig. 5 is assumed to have a 3-hr duration, whereas the contours in Fig. 8 determine each sea state exposure based on the long-term environmental variability. But the sea states leading to appreciable failure probabilities in Fig. 5 would be expected to have much shorter exposures out of the entire 300-year effective exposure, based on the long-term environmental variability model, as reflected by the lower failure probabilities for these sea states from the RBRCs and MCS.

Considering the sea states identified by the largest most-likely extreme relative velocity and bending moment responses at the panel location offers mixed results. The contours of most-likely extreme relative velocity responses certainly approximate the range of sea states leading to high failure probabilities, but not as precisely as the RBRCs in Fig. 4. On the other hand, the contours of most-likely bending moment responses at the panel location give no meaningful insight into sea states leading to the worst panel responses, though it was noted in Seyffert et al. (2019b) the panels were more susceptible to pure lateral load-induced failures (excited by the relative velocity) than pure in-plane load-induced failures (excited by the bending moment).

Sea states identified by the N-year IFORM environmental contours paired with the most-likely extreme relative velocity and bending moment response contours offers interesting, and somewhat diverging conclusions. The 300-year IFORM contour does not identify sea states which lead to appreciable panel failure probabilities, since the range of sea states leading to the largest most-likely extreme relative velocity values generally fall inside of the 300-year IFORM contour. It is only sea states that lead to less extreme relative velocity values that intersect with this 300-year contour, meaning that the identified sea states are not very relevant for panel failure.

The 30-year and 10-year IFORM contour intersections with the contours of most-likely extreme relative velocity responses identify sea states which are much more relevant to panel failure than the 300-year IFORM contour. The 10-year IFORM contour paired with the contours of most-likely extreme relative velocity responses at the panel location identifies sea states that give at minimum 88% of the maximum failure probability for all panel designs. Such an identification of sea states is also quite useful to designers when designing a testing regime. But this result offers a conundrum, that being: what is the appropriate N-year environmental contour to use when examining extreme responses of a system with a M-year lifetime? The *a posteriori* examination of these environmental contours suggests that 10-year IFORM contour identifies more relevant sea states for panel failure than the 300 or 30-year contour. But environmental contours are used when there is not such detailed system response information to determine which return period contour is most relevant for the system response. Certainly the 30-year contour might seem more relevant to examine a system with a 30-year lifetime (before the additional risk factors are applied). But this analysis shows that is not necessarily the case.

This limitation of knowing which return period is most relevant for evaluating system reliability does not pose a challenge for the RBRCs presented in Fig. 4 because the long-term environmental variability along with an applied risk parameter are taken into account to construct those contours. For all three panel designs, the RBRCs give the best identification of relevant sea states for panel reliability of all methods as compared to the brute-force MCS. In addition to identifying relevant sea states, these contours give a low-order estimate of the panel reliability, at least enough to rank relative performance between designs. In terms of designing a testing regime for use in a higher-fidelity model, either physical or numerical, these RBRCs can help focus tests on the most relevant sea states for system performance.

9. Conclusions

This paper established a method to construct response-based reliability contours (RBRCs) for complex marine systems excited by

combined loading effects using indicators of extreme behavior and extreme value theory. As an example, these RBRCs were constructed to identify sea states which are most relevant for stiffened panel failure for three possible panel designs on the David Taylor Model Basin Vessel 5415. For each panel design, these RBRCs identified a sea state which excited a failure probability at least 95% of the maximum failure probability expected from brute-force Monte Carlo Simulations taking into account both short-term response variability and long-term environmental variability over all possible operational profiles. In general, this offers a major advantage when determining a testing regime to evaluate the reliability or performance of a marine system. Based on the RBRCs for these panel designs, an engineer could easily identify relevant sea states to test the panel performance without wasting computational effort on irrelevant sea conditions.

This paper also investigated the effects of assumptions generally used with environmental contour methods, namely: a constant 3-hr sea state duration, which neglects long-term environmental variability, and ignoring short-term response variability.

The RBRCs constructed assuming a constant 3-hr sea state duration can identify relevant sea states for testing a design response, but obscure the risk profile associated with such a sea state occurrence based on the design lifetime. Ignoring the effects of short-term response variability was examined by constructing contours of the most-likely extreme load effect which is relevant for system failure, in this case relative velocity at the panel location. For some panel designs, particularly the panels with a worse overall performance, these contours also identified relevant sea states for panel failure. Such an approach offers a potential solution when a design limit state is unknown but important load effects which affect system performance *are* known.

Finally, the paper examined whether IFORM environmental contours paired with the contours of the most-likely extreme load effect identified the most relevant sea states for stiffened panel collapse. As the system lifetime was set at 30 years with an applied risk parameter leading to a 300-year effective exposure, a 300-year and 30-year IFORM were examined, along with a 10-year contour. Surprisingly the 10-year contour paired with the contours of the most-likely extreme relative velocity response at the panel location identified the most relevant sea states of all the IFORM contours. The ambiguity of choosing the “correct” return period to examine a system with a given lifetime exposure over many potential operational profiles makes applying environmental contours to identify relevant sea states for a particular design response difficult.

In general, the RBRCs were most effective at identifying sea states most relevant to the system performance, here the probability of stiffened ship panel collapse, when taking into account both short-term response variability and long-term environmental variability. The superior performance of the RBRCs over the other low-order methods was most pronounced for the panels with the lowest failure probabilities, indicating that the RBRCs can also be used to identify sea states that excite rare responses. By employing indicators of extreme response behaviors, sea states which are expected to lead to the most interesting system responses can quickly be identified. In this way, a testing regime can be efficiently defined so that resources are devoted to operational profiles which are expected to lead to the worst-case system responses.

Declaration of Competing Interest

The authors have no competing interests to declare.

Acknowledgments

The authors thank Ms. Kelly Cooper and the Office of Naval Research for their support for this research which is funded under the Naval International Cooperative Opportunities in Science and Technology Program (NICOP: N00014-15-1-2752). The authors also

thank the anonymous reviewers for their helpful suggestions and comments.

Supplementary material

Supplementary material associated with this article can be found, in the online version, at [10.1016/j.apor.2020.102332](https://doi.org/10.1016/j.apor.2020.102332)

References

- Ashe, G., Cheng, F., Kaeding, P., Kaneko, H., Dow, R., Broekhuijsen, J., Pegg, N., Fredriksen, A., de Francisco, F., Leguen, J., Hess, P., Gruenitz, L., Jeon, W., Kaneko, H., Silva, S., Sheinberg, R., 2009. Committee V.5 - Naval Ship Design. Technical Report. 17th International Ship and Offshore Structures Congress.
- Baarholm, G.S., Haver, S., Økland, O.D., 2010. Combining contours of significant wave height and peak period with platform response distributions for predicting design response. *Mar. Struct.* 23, 147–163. <https://doi.org/10.1016/j.marstruc.2010.03.001>.
- Baarholm, G.S., Moan, T., 2000. Estimation of nonlinear long-term extremes of hull girder loads in ships. *Mar. Struct.* 13, 495–516. [https://doi.org/10.1016/S0951-8339\(00\)00060-5](https://doi.org/10.1016/S0951-8339(00)00060-5).
- Bitner-Gregersen, E., 2010. Uncertainties of joint long-term probabilistic modelling of wind sea and swell. Proceedings of the 29th International Conference on Ocean, Offshore and Arctic Engineering. <https://doi.org/10.1115/omae2010-20682>.
- Chai, W., Leira, B.J., 2018. Environmental contours based on inverse SORM. *Mar. Struct.* 60 (March), 34–51. <https://doi.org/10.1016/j.marstruc.2018.03.007>.
- Derbanne, Q., de Hauteclouque, G., Dumont, M., 2017. How to account for short-term and long-term variability in the prediction of the 100 years response? Proceedings of the 36th International Conference on Ocean, Offshore and Arctic Engineering. <https://doi.org/10.1115/omae2017-61701>.
- DNV-GL, 2010. Environmental Conditions and Environmental Loads. Technical Report. Recommended Practice DNV-RP-C205.
- DNV-GL, 2017. Modelling and Analysis of Marine Operations. Technical Report. Recommended Practice DNV-RP-H103.
- Fujimura, K., Kiureghian, A.D., 2007. Tail-equivalent linearization method for nonlinear random vibration. *Probab. Eng. Mech.* 22, 63–76. <https://doi.org/10.1016/j.probgmech.2006.08.001>.
- Fukasawa, T., Kawabe, H., Moan, T., 2007. On extreme ship response in severe short-term sea state. *Advancements in Marine Structures - Proceedings of MARSTRUCT 2007, The 1st International Conference on Marine Structures*. pp. 33–40.
- Gouldby, B., Wyncoll, D., Panzeri, M., Franklin, M., Hunt, T., Hames, D., Tozer, N., Hawkes, P., Dornbusch, U., Pullen, T., 2017. Multivariate extreme value modelling of sea conditions around the coast of England. Proceedings of the Institution of Civil Engineers - Maritime Engineering 170 (1), 3–20. <https://doi.org/10.1680/jmaen.2016.16>.
- Haselsteiner, A.F., Ohlendorf, J.-H., Wosniok, W., Thoben, K.-D., 2017. Deriving environmental contours from highest density regions. *Coastal Eng.* 123, 42–51. <https://doi.org/10.1016/j.coastaleng.2017.03.002>.
- Haver, S., 1987. On the joint distribution of heights and periods of sea waves. *Ocean Eng.* 14 (5), 359–376. [https://doi.org/10.1016/0029-8018\(87\)90050-3](https://doi.org/10.1016/0029-8018(87)90050-3).
- Haver, S., Kleiven, G., 2004. Environmental contour lines for design purposes: why and when? Proceedings of the 23rd International Conference on Ocean, Offshore and Arctic Engineering. pp. 337–345.
- Haver, S., Winterstein, S.R., 2008. Environmental contour lines: a method for estimating long term extremes by a short term analysis. *Transactions - Society of Naval Architects and Marine Engineers* 116.
- Hughes, O.F., 1983. Ship structural design: A Rationally-Based, computer-Aided optimization approach. The Society of Naval Architects and Marine Engineers.
- Huseby, A., Vanem, E., Natvig, B., 2013. A new approach to environmental contours for ocean engineering applications based on direct monte carlo simulations. *Ocean Eng.* 60, 124–135. <https://doi.org/10.1016/j.oceaneng.2012.12.034>.
- Huseby, A.B., Vanem, E., Natvig, B., 2014. A new Monte Carlo method for environmental contour estimation. ESREL 2014. European Safety and Reliability Association (ESRA).
- Huseby, A.B., Vanem, E., Natvig, B., 2015. Alternative environmental contours for structural reliability analysis. *Struct. Saf.* 54, 32–45. <https://doi.org/10.1016/j.strusafe.2014.12.003>.
- IACS, 2001. Standard wave data. International Association of Classification Societies Ltd., London. (34), 1–4.
- Jonathan, P., Ewans, K., Flynn, J., 2014. On the estimation of ocean engineering design contours. *J. Offshore Mech. Arct. Eng.* 136 (4). <https://doi.org/10.1115/1.4027645>.
- Kim, D.-H., Engle, A.H., Troesch, A.W., 2011. Estimates of long term combined wave bending and whipping for two alternative hull forms. *Transactions - Society of Naval Architects and Marine Engineers* 120.
- Lutes, L.D., Winterstein, S.R., 2016. A dynamic inverse FORM method: design contours for load combination problems. *Probab. Eng. Mech.* 44, 118–127. <https://doi.org/10.1016/j.probgmech.2015.10.001>.
- NORSOK N-003, 2017. Technical Report. NORSOK Standard N-003:2017: Actions and action effects.
- Ochi, M.K., 1990. Applied probability & stochastic processes in engineering & physical sciences. Wiley series in probability and mathematical sciences.
- Ross, E., Astrup, O.C., Bitner-Gregersen, E., Bunn, N., Feld, G., Gouldby, B., Huseby, A., Liu, Y., Randell, D., Vanem, E., Jonathan, P., 2020. On environmental contours for marine and coastal design. *Ocean Eng.* 195, 106194. <https://doi.org/10.1016/j.oceaneng.2019.106194>.
- Seyffert, H.C., 2018. Extreme Design Events due to Combined, Non-Gaussian Loading. The University of Michigan.
- Seyffert, H.C., Kana, A.A., Troesch, A.W., 2019. Design contours for complex marine systems. *Practical Design of Ships and Other Floating Structures*.
- Seyffert, H.C., Kim, D.-H., Troesch, A.W., 2016. Rare wave groups. *Ocean Eng.* 122, 241–252. <https://doi.org/10.1016/j.oceaneng.2016.05.053>.
- Seyffert, H.C., Troesch, A.W., Collette, M.D., 2019. Combined stochastic lateral and in-plane loading of a stiffened ship panel leading to collapse. *Mar. Struct.* 67. <https://doi.org/10.1016/j.marstruc.2019.04.008>.
- Sødahl, N., Hagen, Ø., Steinkjer, O., Chezhian, M., 2006. Calculation of extreme nonlinear riser response. DOT 2006, Houston, USA.
- Vanem, E., 2017. A comparison study on the estimation of extreme structural response from different environmental contour methods. *Mar. Struct.* 56, 137–162. <https://doi.org/10.1016/j.marstruc.2017.07.002>.
- Vanem, E., Bitner-Gregersen, E., 2012. Stochastic modelling of long-term trends in the wave climate and its potential impact on ship structural loads. *Appl. Ocean Res.* 37, 235–248. <https://doi.org/10.1016/j.apor.2012.05.006>.
- Vanem, E., Guo, B., 2019. Comparison of the Environmental Contour Method and Response-Based Analysis Using Response Emulator for Estimating Extreme Ship Responses. Proceedings of the 38th International Conference on Ocean, Offshore and Arctic Engineering. <https://doi.org/10.1115/OMAE2019-95098>.
- Vanem, E., Guo, B., Ross, E., Jonathan, P., 2020. Comparing different contour methods with response-based methods for extreme ship response analysis. *Mar. Struct.* 69. <https://doi.org/10.1016/j.marstruc.2019.102680>.
- Wang, S., Wang, X., Woo, W.L., 2018. A comparison of response-based analysis and environmental contour methods for FPSO green water assessment. Proceedings of the 37th International Conference on Ocean, Offshore and Arctic Engineering.
- Winterstein, S.R., Ude, T., Cornell, C., Bjerager, P., Haver, S., 1993. Environmental parameters for extreme response: inverse FORM with omission factors. *Proc. of Intl. Conf. on Structural Safety and Reliability (ICOSAR93)*.